Gastroenterol Hepatol. 2019;42(2):117–126

Gastroenterología y Hepatología

www.elsevier.es/gastroenterologia

REVIEW

Endoscopic microanatomy of the normal gastrointestinal mucosa with narrow band technology and magnification

Hugo Uchima[a,b,*], **Kenshi Yao**[c]

[a] *Department of Endoscopy, Hospital Universitari Doctor Josep Trueta, Girona, Spain*
[b] *Department of Endoscopy, Teknon Medical Center, Barcelona, Spain*
[c] *Department of Endoscopy, Fukuoka University Chikushi Hospital, Fukuoka, Japan*

Received 19 March 2018; accepted 1 October 2018

KEYWORDS
Endoscopy;
Endoscopic microanatomy;
Image-enhanced endoscopy;
Magnifying endoscopy;
Narrow-band imaging;
Blue light imaging

Abstract The development of high-definition endoscopes with optical zoom, along with the use of the digital chromoendoscopy and staining, has given endoscopists the possibility to study the microanatomy of the gastrointestinal mucosa in vivo. The recognition of the changes in the microstructure of the surface and microvascular architecture such as those that occur in neoplastic lesions allow us to characterize these lesions in order to decide on the best course of clinical action. The current greater availability of endoscopes with optical zoom in western countries has allowed the use of this technology in routine clinical practice to spread. In this article we review the basic concepts of magnifying endoscopy and the normal endoscopic microanatomy of the oesophageal, gastric, duodenal, ileal and colonic mucosa.

Abbreviations: BLI, blue light imaging/blue laser imaging; EGJ, esophagogastric junction; IPCL, intrapapillary capillary loops; DWI, dual wavelength imaging with bandwidth narrowing; M-DWI, magnifying endoscopy with dual wavelength imaging; ME, magnifying endoscopy; WLI, white light-imaging; MS, microsurface; MV, microvascular; NBI, narrow band imaging; OE, optical enhancement; SEC, subepithelial capillaries.

* Corresponding author.
E-mail address: huchima.girona.ics@gencat.cat (H. Uchima).

2444-3824/

PALABRAS CLAVE
Endoscopia;
Microanatomía endoscópica;
Imagenología endoscópica;
Endoscopia de magnificación;
Imagen de banda estrecha;
Imagen de luz azul

Microanatomía endoscópica de la mucosa gastrointestinal normal con tecnología de banda estrecha y magnificación

Resumen El desarrollo de endoscopios de alta definición con magnificación óptica, junto a la utilización de la cromoendoscopia digital y de tinción, han permitido el estudio de la microanatomía de la mucosa gastrointestinal en vivo. El reconocimiento de los cambios en el patrón de la microestructura de la superficie y del patrón microvascular como los que se presentan en las lesiones neoplásicas, nos permiten caracterizar estas lesiones para decidir la mejor actuación clínica. Debido a la mayor disponibilidad actual en países occidentales de estos endoscopios con magnificación óptica, su utilización es parte de la práctica clínica habitual cada vez en más centros. Aquí revisaremos los conceptos básicos de la magnificación endoscópica y la microanatomía endoscópica normal de la mucosa esofágica, gástrica, duodenal, ileal y colónica.

Introduction

The development of better endoscopic imaging with magnifying endoscopy has given the endoscopists the possibility to study the microanatomy of the gastrointestinal mucosa in vivo, being possible to evaluate the changes in the microvasculature and the microsurface that occurs in the neoplastic tissue.

By recognition of different microsurface patterns or alterations in the microvasculature the gastrointestinal endoscopist is able to characterize different lesions and to predict the risk of deep (submucosal) invasion which indirectly predicts the risk of lymph node metastases, and thus helping to decide if an endoscopic resection with curative intention could be performed, allowing organ preservation.

Image-enhanced endoscopy (IEE) by using chromoendoscopy (e.g. lugol, acetic acid, indigo carmine, crystal violet) or dual wavelenght imaging with narrow band technology visualized as ''blue light'' (e.g. NBI, BLI, Iscan-OE) are currently an essential part of clinical practice, being of special interest in endoscopic diagnostic and management of pre-malignant lesions and early gastrointestinal cancers.

Many classifications using IEE has been developed for characterization of esophageal, gastric and colonic lesions and to predict their risk of submucosal invasion.[1–3]

The use of magnifying endoscopy, developed in Japan, is spreading to western countries, so gastrointestinal endoscopists should learn this approach, understand the endoscopic microanatomy of the gastrointestinal mucosa and its changes in pathological states such as neoplastic tissue progression.

We will review the basics of the normal microanatomy of the gastrointestinal mucosa evaluated by magnified and endoscopy using the optical narrow band technologies. Summarized in Table 1.

Dual wavelength imaging with bandwidth narrowing/the narrow band technology

Wave-particle duality is one of the characteristics of light. Visible light for the human eye is electromagnetic radiation within a certain portion of the electromagnetic spectrum, usually defined as having wavelengths (the distance between peaks in each wave) in the range of 400–700 nanometres (nm), between the infrared, with longer wavelengths, and the ultraviolet,with shorter wavelengths. This wavelength means a frequency range of roughly 430–750 terahertz (THz). The spectral sensitivity of the light-adapted eye depends on the photopigments in the three kinds of cones with a different absorbance spectrum, called S, M and L (for short, medium, and long wavelengths, ∼420, 530, and 560 nm), the longer wavelength will be seen as red, with the shorter as blue, and in between as green.[4,5]

The biological pigments in the human body can be divided into hematogenous pigments (as hemoglobin), non hematogenous pigments (as melanin) and endogenous minerals (as copper).[6] Hemoglobin is composed of a single protein called globin and a compound called ''heme'', the latter containing iron atoms and the red pigment porphyrin (a metalloporphyrin). The absorption of visible light in metalloporphyrins take place at wavelengths around 400 nm (''blue light'') and 550 nm (''green light''), reflecting the ''red light'' (wavelengths around 700 nm), giving the color to blood. If red light is omitted and only the dual wavelengths green and blue are projected directly to the hemoglobin, it will absorb the blue and green light and no light would be reflected, giving the perception of black.[7] This is the basis of the dual wavelength imaging with narrow band technology (DWI), one of the most important advances in the field of endoscopic imaging. This technology was first developed by Olympus Medical Systems Corp in collaboration with National Cancer Center Hospital East (Tokyo, Japan), introducing in 2005 the narrow band imaging (NBI), an optical digital method of image-enhanced endoscopy based in the narrow band spectrum of light and its effects on the mucosal surface and the hemoglobin of the microvasculature.[8,9]

The gastrointestinal mucosa is a semitransparent and optical turbid medium with small particles such as complex proteins, and cell structures, so when light strikes these particles, it scatters and diffuses. Different light wavelengths have different reflection, depth of propagation, and scattering in the biological tissue. Red light diffuses widely and deeply because of its longer wavelength, compared to blue

Table 1 Normal endoscopic microanatomy. WLI: white light image; M-DWI: magnifying endoscopy with dual wavelength imaging; IPCL, intrapapillary capillary loops.

Organ	Histology	Endoscopic WLI	Endoscopic microvascular M-DWI	Endoscopic microsurface M-DWI
Esophagus	Non-keratinising stratified squamous epithelium with numerous intraepithelial papilla containing IPCL	Smooth and pink mucosa. Palisade vessels at EGJ IPCL might be seen as red dots	IPCL might be seen as brown dots Branching vessels might be cyan	Smooth surface
Gastric Body and Fundus	Gastric pits Straight tubular fundic glands	Red mucosa Collecting venules might be seen as spider shaped red dots	Honeycomb-like pattern of the subepithelial capillaries surrounds each gastric pit. Collecting venules are cyan	Round or oval crypt opening (dark brown) surrounded by a white circular marginal crypt epithelium, in the middle of the gastric pit
Gastric antrum	Coiled pyloric gland in antrum and pylorus Collecting venules are located in the deeper part of the lamina propria	Red mucosa Collecting venules are not usually seen	Coil-shaped subepithelial capillaries. Collecting venules are difficult to discern	Crypt openings are not visualized. Intervening part is surrounded by a regular polygonal or curved marginal crypt epithelium
Duodenum	Villi surrounded by crypts of Lieberkühn	Red mucosa with villi	Loop-shaped capillaries	Regular curved or oval-shaped marginal villous epithelium
Colon	Smooth surface with tubular crypts of Lieberkühn	Red mucosa with grooves (innominate grooves)	Regular or hexagonal honeycomb-like	Regular round pit pattern seen with chromoendoscopy

light that has a short wavelength and propagates shallowly and is scattered over a narrow area.

NBI functions by filtering the illumination light eliminating the red component and by narrowing from 50–70 nm to 20–30 nm the spectral bandwidth of the blue (centered on 415 nm) and green (centered on 540 nm) light, giving a dual wavelength imaging with bandwidth narrowing that can visualize capillary networks clearly. The narrow band blue light delineates in high contrast superficial microvessels, and narrow band green light, that penetrates the tissue over a fairly deep and fairly wide range, delinates in high contrast vessels in the middle layers. The incoming signals from the camera of the endoscope are then combined by the video processor doing specific color allocation to produce a final color image: the narrow band blue image is allocated to the blue and green color channel and the narrow band green image is allocated to the red channel. On the NBI image displayed, the more superficial thin capillary network underneath the epithelium has a brownish appearance and thick deeper blood vessels have a cyan appearance.

Since its launch in 2005, NBI with high definition or magnifying endoscopes has been used worldwide by gastrointestinal endoscopist to improve visualization of the vascular patterns in the superficial part of the mucosa for a better diagnosis, predicting histology, distinguishing between neoplasia and non-neoplasia, and depth of infiltration of early gastrointestinal tumors. Nowadays, new systems similar to NBI, for example the BLI (blue light imaging in Europe and blue laser imaging in Japan, Fujifilm) and i-scan OE (Optical Enhancement system, Pentax) are also available and they seem to be very useful in clinical practice as well.[10–13]

Endoscopic gastrointestinal microanatomy

Endoscopic imaging has been evolving, and nowadays, there are available different endoscopes with high magnification and high resolution power varying according to manufacturers. Magnifying ratio in endoscopy can be a tricky concept as it depends on the size of the monitor. To have an idea, Fujifilm EG-760R has a ''normal'' magnification of 40× in a 19 inch monitor, and the EG-760Z with optical zoom has a medium magnification of 80× and a high magnification of 135× in the same 19 inch monitor, according to the manufacturer, so in this case high magnification would be around 3.5 times higher than ''normal'' magnification.

In Spain the Olympus scopes with near focus (medium magnification) and Fujifilm and Pentax scopes with optical zoom-high magnification are currently available.

If we define the maximal endoscope's resolution as the size of the smallest structure that can be visualized when the endoscope has been brought as close as possible to the object while staying in focus, for targeting the capillaries (microvessels) a resolution of approximately 8 μm is required.[14,15]

With the use of DWI, magnifying endoscopy allows the endoscopist an in vivo study of the microanatomy, by observing the microsurface and the microvascular architecture,

even the red blood cells movement using the maximal resolution power of a high-definition magnification endoscope.[30]

For performing this examination, the use of hood at the tip of the endoscope to fix the distance to the mucosal surface is helpful in order to consistently focus the microstructures at maximal resolution power.[15]

Then we will review the endoscopic microanatomy of the mucosa of the esophagus, stomach, small bowel (duodenum and ileum) and colon, with magnifying endoscopy (ME) and DWI, that we will refer as M-DWI. The recognition of the microsurface (MS) structure and microvascular (MV) architecture has biological significance and clinical implications, specially in the characterization of early gastrointestinal neoplasia, because both the neoplastic vessels and epithelium undergo considerable change during progression to invasive cancer.[16]

Endoscopic microanatomy of the esophageal mucosa

During white light-imaging (WLI) evaluation the esophageal mucosa appears smooth and pink, and the esophagogastric junction (EGJ) appears as an irregular Z-line (ora serrata) demarcating the interface with the redder gastric mucosa. The longitudinal palisade vessels, are relatively large vessels more frequently in the lamina propria rather than in the submucosa at the lower oesophageal sphincter, they are visible at endoscopy and helpful in defining the oesophagogastric junction.

The esophageal mucosa, about 500–800 μm thick, is composed of non-keratinising stratified squamous epithelium (300–500 μm), with a subjacent lamina propria resting on the underlying muscularis mucosae. There are numerous intraepithelial papilla projecting upwards for 2/3 of the total thickness of the epithelium containing intrapapillary vessels called intrapapillary capillary loops (IPCL) arising perpendicularly from the branching vessel network that is located immediately above the muscularis mucosa, in the lamina propria. The IPCL are end capillaries of about 7–10 μm (the minimum to allow the passage of red blood cells) that run adjacent to basement membrane, being affected by alterations in the basal or parabasal layer and reflecting morphological changes of the epithelial papilla. IPCL's morphological changes has an important role in the characterization of early squamous cell carcinoma.[17–19]

The IPCL are identified as red dots under white light and as brown dots with DWI, and the branching vessels are red under white light and cyan under DWI. In Fig. 1A and B we can see this microvascular architecture by using M-DWI.

The observation of the microsurface and microvasculature has clinical implications in the study of Barrett's esophagus, where the normal smooth microsurface of the squamous epithelium of the esophagus is replaced by a columnar epithelium (see Fig. 1C and D). In nondysplastic Barrett's esophagus the surface pattern usually has a regular circular, tubular or ridged/villous pattern. Irregularity in microsurface structure and microvascular architecture are predictors of dysplasia in Barrett's esophagus.[1]

Endoscopic microanatomy of the gastric mucosa

The stomach is a J-shaped dilation of the alimentary canal, it begins at the gastric cardia with gradual histological transition from cardiac glands to the second region, the acid-secreting segment (fundus and body) and then to the final region, corresponding to the antrum and pylorus. The mucosa is lined by a simple layer of columnar epithelial cells (20–40 μm height), that invaginates into the mucosa increasing the surface area of the gastric lining, forming gastric pits (foveolae), which are shallowest in the cardiac region and deepest in the pyloric region. The gastric pits provide the gastric glands of the lamina propria acces to the gastric lumen (about 4 or 5 glands per pit).

Body and fundic mucosa have the same histology characterized by straight and simple tubular glands known as fundic (oxyntic) glands. This mucosal thickness varies from 400 μm to 1500 μm, with the ratio of pit and proper gland thickness being 1:2 in the gastric fundic gland mucosa and 1:1 in the gastric pyloric gland mucosa. Immediately deep to the basement membrane of the epithelial layer lies the lamina propria, containing the subepithelial capillaries (SEC), arising from branch from submucosal arterioles penetrating the muscularis mucosa. The SEC are distributed from the base of the glands toward the epithelium as they repeatedly anastomose with each other surrounding the glands, forming a regular honeycomb like subepithelial capillary network (SECN) in the gastric fundic gland mucosa and a coil-shaped SECN in the gastric pyloric gland feeding into subepithelial collecting venules (CV). The CVs travel obliquely downwards within the lamina propria to the submucosal venules.

The narrow band blue light contributes to visualization of subepithelial capillary network (SECN) and the mucosal microsurface structure. The narrow band green light contributes to visualization of part of the SECN and to visualization of the collecting venules (CVs), located deeper than the subepithelial capillaries.

In the fundic gland mucosa, CVs are seen red under white light or cyan under DWI.

Using M-DWI, the SECs are visualized as brownish polygonal (mainly hexagonal) closed loops of subepithelial capillaries anastomosing with each other, giving a of honeycomb-like pattern. The marginal crypt epithelium (MCE) is seen as a semitransparent white border surrounding the crypt opening (CO) which is seen as a dark brown oval-shaped hole. The area between crypt and crypt is called the intervening part (IP). An scheme and a picture of the normal fundic glandular mucosa are shown in Fig. 2A–D.

The antrum and pylorus contains the extensively coiled pyloric glands. Mucosal capillaries are relatively sparse compared with the fundic gland mucosa. At the lamina propria, some capillaries branch straight from arterioles beneath the muscularis mucosa and some from arterioles that penetrate the muscularis mucosa and then branch out. Capillaries repeatedly anastomose with each other reaching the subepithelial region forming a coil-shaped subepithelial capillary network (SECN), and then feed into collecting venules (CVs) in a relatively deep part of the lamina propria.

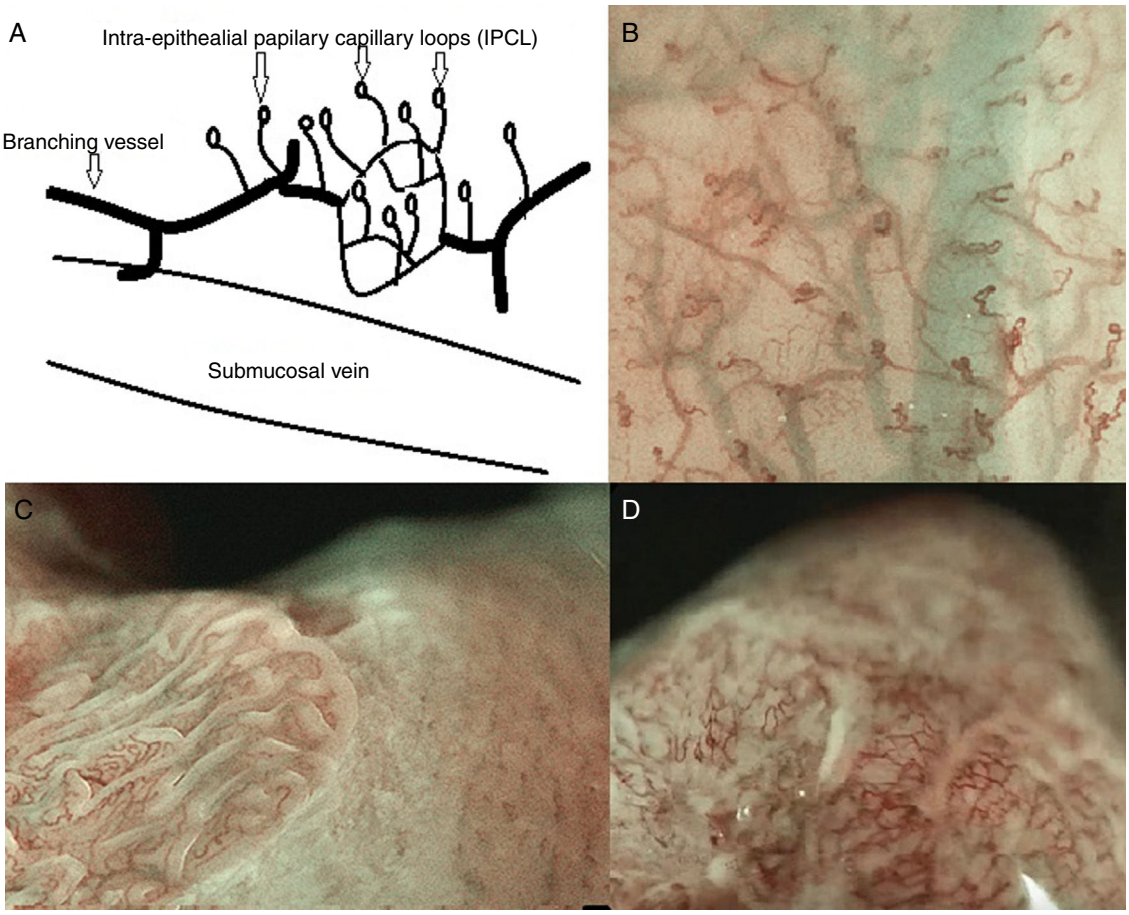

Figure 1 (A) Scheme showing the microvascular architecture of the mucosa, that drains in the submucosal vein. The IPCL run adjacent to basement membrane of the esophageal squamous epithelium, and can reflect morphological changes of the epithelial papilla, for example in cases of epithelial cancer (squamous cell carcinoma). Figure modified from Inoue et al. [18]. (B) Normal esophageal mucosa microanatomy under BLI (blue light imaging, Fujifilm) magnifying observation. The Branching vessels are cyan, and the small capillaries are brown. (C) Columnar-lined epithelium of non-dysplastic Barrett's esophagus is seen in contrast to the whitish esophageal squamous epithelial around. The microsurface structure shows a regular (ridged and tubular) mucosal pattern without irregularities (BLI with medium magnification observation). (D) BLI with high magnification of Barrett's adenocarcinoma with infiltration of 500 μm into the submucosal layer. Irregular microvessels are seen and it is not possible to recognize mucosal pattern.

In the gastric pyloric gland mucosa, CVs are difficult to discern even using M-DWI, because they are located deep to the superficial layer of the mucosa.

Using M-DWI, the SEC are visualized as brownish coil-shaped open loops, and rarely with a reticular pattern.

The microsurface structure of the gastric pyloric gland mucosa is made up of the marginal crypt epithelium (MCE) surrounding the intervening part (IP), the MCE morphology is usually polygonal but may be curved or linear. Crypt openings are not visualized in the antrum because crypts running perpendicular to the mucosal surface are uncommon.[7,15,17,20] An scheme and a picture of the normal pyloric glandular mucosa are shown in Fig. 3A–D.

The light blue crest sign (LBC, Fig. 4A), described first by Uedo et al.[21] is defined as a fine blue white line on the crests of the epithelial surface/gyri and it is an optical marker for the endoscopic diagnosis of intestinal metaplasia, being well correlated with histology. This phenomenon involves strong reflection of short wavelength narrow-band blue light, probably by the microvilli of the brush borders of the areas of intestinal metaplasia. The same phenomenon is seen in the epithelial margins of small bowel mucosa.

The white opaque substance (WOS, Fig. 4B), described by Yao et al.[22] is another phenomenon that may be present in gastric epithelial neoplasia and intestinal metaplasia. It is visualized using either normal white light or blue light, and indicates the accumulation of lipid micro-droplets in the superficial (intraepithelial and subepithelial) part of gastric epithelial neoplasias (adenoma and cancer), due to an impaired mitochondrial oxidation, lipoprotein excretion and lipid degradation. The lipid drops have a higher reflective index than organelles and organic components of the tissue, it follows that projected light is strongly scattered and reflected, this strong backward scattering and reflection of light is recognized as white coloration by the human eye.[23,24] Thus, WOS is another optical marker for intestinal metaplasia as well as LBC[25] and it may help for discriminating

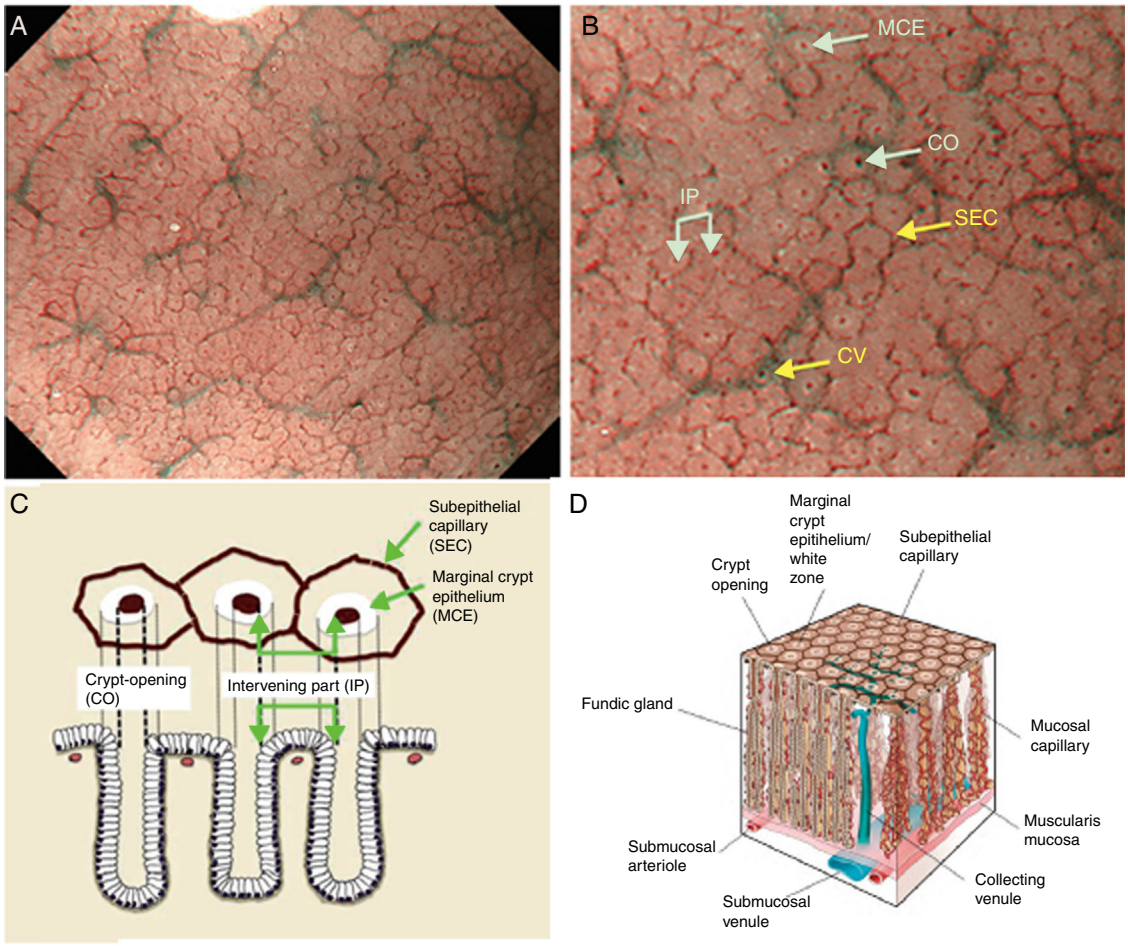

Figure 2 (A) Normal gastric fundic gland mucosa microanatomy under NBI (narrow-band imaging) magnifying observation. (B) Microvascular architecture: honeycomb-like subepithelial capillary network (SECN) and collecting venules (CV). Microsurface structure: oval crypt opening (CO) in dark brown and white circular marginal crypt epithelium (MCE). The area between crypt and crypt is called the intervening part (IP). (C, D) Scheme of the normal microanatomy of the fundic gland mucosa and correlation between visualized endoscopic mucosa microanatomy and histological findings.
Source: Modified from Refs. [2,20].

adenoma (with a regular WOS) from carcinoma (irregular WOS) when using M-DWI.[22]

Irregularity in microvascular and microsurface patterns present within the demarcation line are predictors of gastric neoplasia (Fig. 4C and D).[15,20]

Endoscopic microanatomy of the mucosa of duodenum and ileum

The duodenum, the most proximal portion of the small bowel, was so named because it is approximately 12 fingers in breadth. It has a mucosa made up of a single layer epithelium, a supporting lamina propria and the muscularis mucosae. The epithelium and lamina propria form leaf-like (spade-like) intraluminal projections called villi (lining the entire small bowel), covered by a brush border at the apical surface, surrounded by tubular invaginations known as crypts of Lieberkühn, that extend to the muscularis mucosa. The lamina propria contains a centrally located lymphatic capillary (lacteal) and an arteriovenous capillary network.

The villi in the duodenal bulb have a distorted appearance and tend to be short, in contrast, the villi of the distal duodenum are tall, slender, and regular.

Under endoscopic examination with M-DWI, the microsurface structure shows a regular curved (if observed obliquely) or oval-shaped (if observed perpendicular) marginal villous epithelium (MVE), visualized as a white belt-like structure. Light blue crest can be visualized in the periphery of the normal duodenal and ileal MVE, depending on the direction of the observation (reflection of the ''blue light'').

The crypt openings normally are not visualized, because they are deeper than the villi.

The microvascular architecture shows loop-shaped capillaries located inside the villi bordering of the MVE forming anastomoses inside the villi, the regular villous subepithelial capillary network. At times they can be observed flowing into the villous venules in the deep part (Fig. 5A).[26]

In celiac disease, when there is atrophy of the duodenal villi, the disappearance of the microstructure becomes evident (Fig. 5B).[27–29]

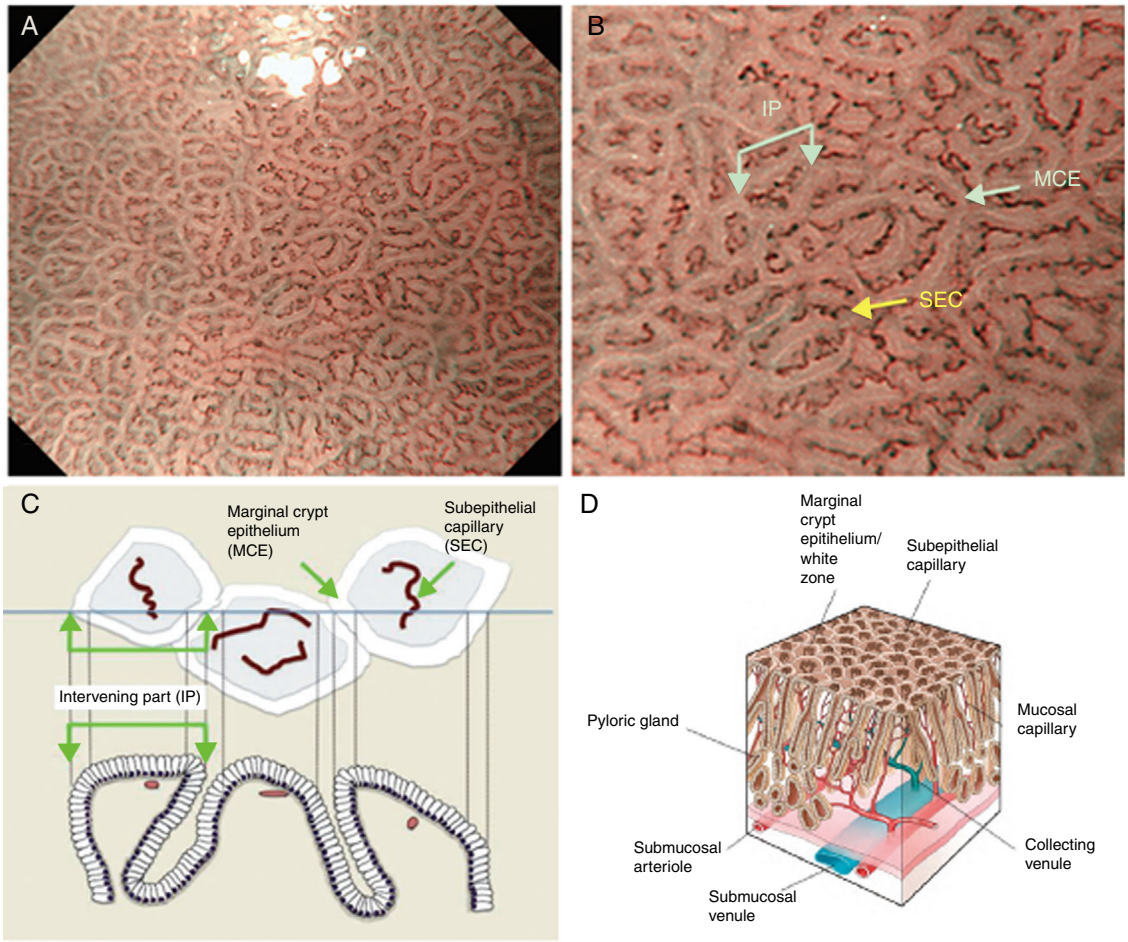

Figure 3 (A) Normal gastric pyloric gland mucosa microanatomy under NBI (narrow-band imaging) magnifying observation. (B) Microvascular architecture: coil-shaped subepithelial capillary (SEC). The collecting venules are difficult to discern because they are located in the deeper part of the lamina propria mucosae. Microsurface structure: regular polygonal or curved marginal crypt epithelium (MCE). Crypt opening is not visualized at the surface. The intervening part (IP) is surrounded by the MCE. (C, D) Scheme of the normal microanatomy of the pyloric gland mucosa and correlation between visualized endoscopic mucosa microanatomy and histological findings.
Source: Modified from Refs. [2,20].

The terminal ileum shows a similar microsurface structure and microvascular architecture to the duodenum (Fig. 5C).

Endoscopic microanatomy of the mucosa of colon and rectum

The mucosa of the large intestine is a relatively smooth surface with the innominate grooves being visible on endoscopic inspection. It is characterized by the presence of crypts of Lieberkühn and it is composed of a simple columnar epithelium, lamina propria with capillaries and associated venules, and muscularis mucosa at the lower border. There are some lymphatics in the lamina propria that are restricted to a region immediately superficial to the muscularis mucosae that penetrates into the submucosa forming numerous solitary lymphatic nodules. In the submucosa, there are blood vessels, lymphatics and Meissner submucosal plexus, and the submucosal veins could be seen through the transparent epithelium.

The crypts of Lieberkühn are tubular and dip to the muscularis mucosae, giving a ''rack of test-tubes'' appearance when we see the normal pit pattern.

With high definition M-DWI it is possible to visualize a regular hexagonal or honeycomb-like subepithelial capillary network in each part of the large intestine, except for the rectum,[30] and with chromoendoscopy a regular round pit pattern (Kudo's pit pattern I) is found in the normal mucosa, as seen in Fig. 6.

In clinical practice, the study of the microcapillary pattern by using ''blue light'' and the use of chromoendoscopy (e.g. crystal violet, indigo carmine) to asses the surface structure (crypts) of colonic lesions is used to characterize neoplastic lesions and predict the grade of submucosal invasion by using classifications such as the Japanese NBI Expert Team (JNET) classification and the pit pattern.[3,31–33] NICE classification can be used with DWI without magnification (Fig. 7).

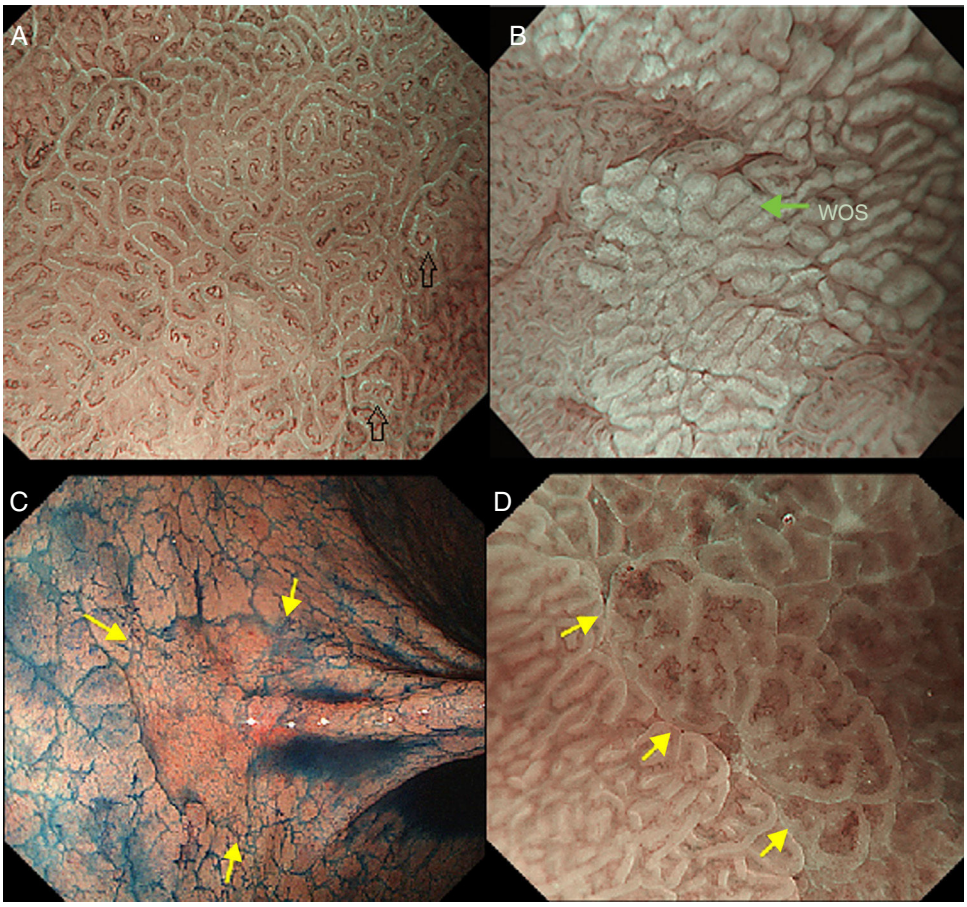

Figure 4 (A) Light blue crest (LBC). BLI (blue light imaging, Fujifilm) magnifying observation showing numeorus fine bluish (light cyan) lines in the antrum, as for example, those signalized by arrows. This phenomenon (reflection of the blue light) is characteristic of intestinal metaplasia in the stomach, but is also present in the normal mucosa of the small bowel, as seen in duodenum or ileum. (B) White opaque substance (WOS). NBI (narrow-band imaging, Olympus) magnifying observation of the gastric mucosa showing an white opaque coloration (arrow) due to light strong scattering and reflection, it is produced by accumulation of lipid droplets within the surface epithelium in the stomach. Picture from Ref. [20]. (C) Conventional white-light endoscopic findings with the dye (indigocarmine)-spraying method. After the dye is sprayed, the lesion can be clearly visualized. As the margin of the lesion (arrows) shows irregularity, this finding is compatible with the diagnosis of early gastric cancer. (D) Magnifying endoscopic findings with narrow-band imaging of the same lesion. A clear demarcation line (arrows) is noted at the margin. Both irregular microvascular and irregular microsurface patterns are present within the demarcation line. Histological findings of endoscopically resected specimen showed well- to poorly differentiated adenocarcinoma limited to the mucosa. Pictures C and D from Ref. [2].

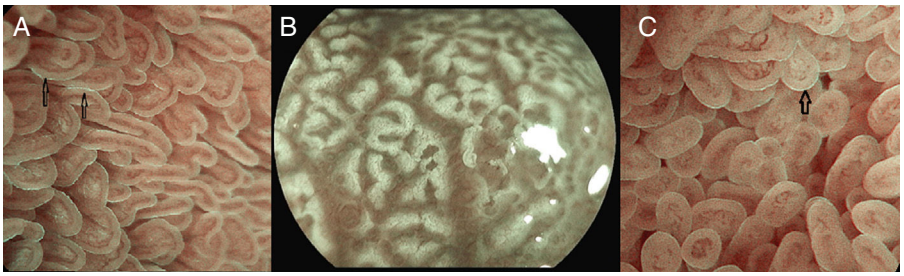

Figure 5 (A) Normal duodenal mucosa under BLI (Blue light imaging) magnifying observation. The blue light crest (LBC) is present (arrows). (B) Atrophy of duodenal villi under BLI (blue light imaging) magnifying observation. Loss of microsurface structure (absence of villi). (C) Normal mucosa of ileum, under BLI (blue light imaging) magnifying observation. The blue light crest (LBC) is present (arrow).

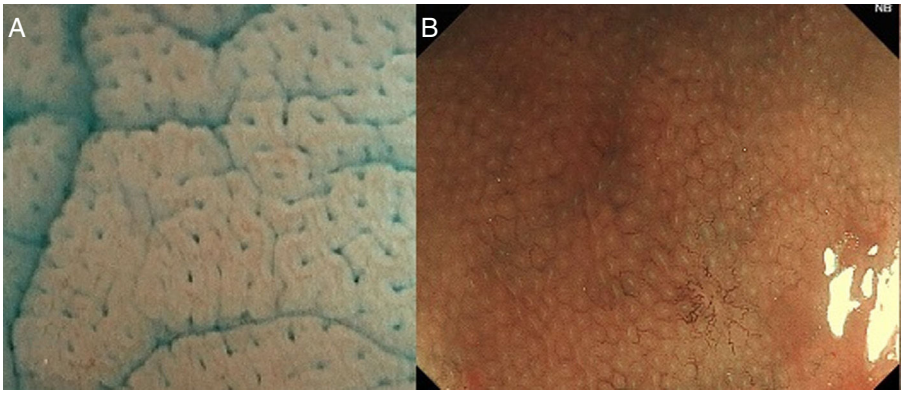

Figure 6 (A) Normal round pit pattern under magnified observation with indigo carmine. (B) Honeycomb-like appearance of the subepithelial capillary network in colon, under M-DWI.

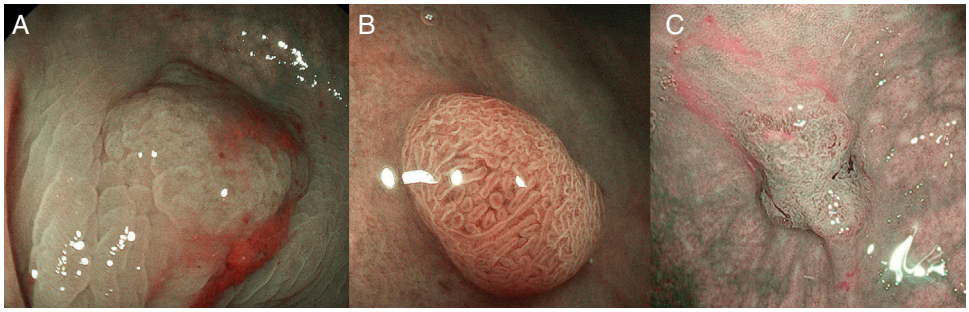

Figure 7 (A) NICE 1: hyperplastic lesion with same color than background and none vessels coursing across the lesion. (B) NICE 2: adenoma with low grade dysplasia with a browner color than background, with a regular surface pattern and regular vessels. (C) NICE 3: deep submucosal invasive adenocarcinoma in a lesion with a central demarcated area with amorphous surface pattern and disrupted vessels.

It is important to remember that pit pattern should be evaluated with chromoendoscopy using indigo carmine or crystal violet. M-DWI allows us to describe the surface pattern as regular, irregular or absent, but not the pit pattern properly.

Conflict of interest

The authors declare no conflict of interest.

References

1. Sharma P, Bergman JJGHM, Goda K, Kato M, Messmann H, Alsop BR, et al. Development and validation of a classification system to identify high-grade dysplasia and esophageal adenocarcinoma in Barrett's esophagus using narrow-band imaging. Gastroenterology. 2016;150:591–8.
2. Muto M, Yao K, Kaise M, Kato M, Uedo N, Yagi K, et al. Magnifying endoscopy simple diagnostic algorithm for early gastric cancer (MESDA-G). Dig Endosc. 2016;28:379–93.
3. Sano Y, Tanaka S, Kudo SE, Saito S, Matsuda T, Wada Y, et al. Narrow-band imaging (NBI) magnifying endoscopic classification of colorectal tumors proposed by the Japan NBI expert team. Dig Endosc. 2016;28:526–33.
4. Hall J. The eye: II. Receptor and neural function of the retina. In: Hall J, editor. Guyton and hall textbook of medical physiology. 13th ed. United States of America: Elsevier; 2016. p. 647–60.
5. Connors BW. Sensory transduction. In: Boron W, editor. Medical physiology. 3rd ed. UK: Elsevier Inc.; 2017. p. 353–89.
6. Orchard GE. Pigments and minerals. In: Suvarna K, Layton C, Bancroft J, editors. Bancroft's theory and practice of histological techniques. 7th ed. UK: Elsevier Ltd.; 2017. p. 239–70.
7. Yao K, Takaki Y, Matsui T, Iwashita A, Anagnostopoulos GK, Kaye P, et al. Clinical application of magnification endoscopy and narrow-band imaging in the upper gastrointestinal tract: new imaging techniques for detecting and characterizing gastrointestinal neoplasia. Gastrointest Endosc Clin N Am. 2008;18:415–33.
8. Gono K. Narrow band imaging: technology basis and research and development history. Clin Endosc. 2015;48:476–80.
9. Du Le V, Wang Q, Gould T, Ramella-Roman J, Pfefer J. Vascular contrast in narrow-band and white light imaging. Appl Opt. 2014;53:4061–71, 20.
10. Kaneko K, Oono Y, Yano T, Ikematsu H, Odagaki T, Yoda Y, et al. Effect of novel bright image enhanced endoscopy using blue laser imaging (BLI). Endosc Int Open. 2014;2:E212–9.
11. Neumann H, Fujishiro M, Wilcox M, Mönkemüller K. Present and future perspectives of virtual chromoendoscopy with i-scan and optical enhancement technology. Dig Endosc. 2014;26 Suppl. 1:43–51.
12. Tajiri H, Kato M, Tanaka S, Saito Y, Muto M. NBI/BLI atlas. Tokyo: Nihon Medical Center; 2014.
13. Nagao M, Nishikawa J, Ogawa R, Sasaki S, Nakamura M, Nishimura J, et al. Evaluation of the diagnostic ability of optical enhancement system in early gastric cancer demarcation. Gastroenterol Res Pract. 2016;2016:2439621.

14. Yabe H. Magnifying ratio and resolution of electronic endoscopes. Dig Endosc. 2002;14 Suppl. 1:S88–90.
15. Yao K. Zoom gastroscopy. Tokyo: Springer; 2014.
16. Kumagai Y, Toi M, Inoue H. Dynamism of tumour vasculature in the early phase of cancer progression: outcomes from oesophageal cancer research. Lancet Oncol. 2002;3: 604–10.
17. Shepherd N, Warren B, Williams G, Greenson J, Lauwers G, Novelli M. Morson and Dawson's gastrointestinal pathology. 5th ed. London: Blackwell Publishing; 2013.
18. Inoue H, Kaga M, Ikeda H, Sato C, Sato H, Minami H, et al. Magnification endoscopy in esophageal squamous cell carcinoma: a review of the intrapapillary capillary loop classification. Ann Gastroenterol. 2015;28:41–8.
19. Inoue H, Honda T, Yoshida T, Nishikage T, Nagahama T, Yano K, et al. Ultra-high magnification endoscopy of the normal esophageal mucosa. Dig Endosc. 1996;8:134–8.
20. Yao K. Clinical application of magnifying endoscopy with narrow-band imaging in the stomach. Clin Endosc. 2015;48:481–90.
21. Uedo N, Ishihara R, Iishi H, Yamamoto S, Yamada T, Imanaka K, et al. A new method of diagnosing gastric intestinal metaplasia: narrow-band imaging with magnifying endoscopy. Endoscopy. 2006;38:819–24.
22. Yao K, Iwashita A, Tanabe H, Nishimata N, Nagahama T, Maki S, et al. White opaque substance within superficial elevated gastric neoplasia as visualized by magnification endoscopy with narrow-band imaging: a new optical sign for differentiating between adenoma and carcinoma. Gastrointest Endosc. 2008;68:574–80.
23. Yao K, Iwashita A, Nambu M, Tanabe H, Nagahama T, Maki S, et al. Nature of white opaque substance in gastric epithelial neoplasia as visualized by magnifying endoscopy with narrow-band imaging. Dig Endosc. 2012;24:419–25.
24. Enjoji M, Kohjima M, Ohtsu K, Matsunaga K, Murata Y, Nakamuta M, et al. Intracellular mechanisms underlying lipid accumulation (white opaque substance) in gastric epithelial neoplasms: a pilot study of expression profiles of lipid-metabolism-associated genes. J Gastroenterol Hepatol. 2016;31:776–81.
25. Kanemitsu T, Yao K, Nagahama T, Imamura K, Fujiwara S, Ueki T, et al. Extending magnifying NBI diagnosis of intestinal metaplasia in the stomach: the white opaque substance marker. Endoscopy. 2017;49:529–35.
26. Yao K. Normal duodenal mucosa. In: Muto M, Yao K, Sano Y, editors. Atlas of endoscopy with narrow band imaging. Tokyo, Japan: Springer; 2015. p. 147.
27. De Luca L, Ricciardiello L, Rocchi MB, Fabi MT, Bianchi ML, de Leone A, et al. Narrow band imaging with magnification endoscopy for celiac disease: results from a prospective, single-center study. Diagn Ther Endosc. 2013;2013:580526.
28. Dutta AK, Sajith KG, Shah G, Pulimood AB, Simon EG, Joseph AJ, et al. Duodenal villous morphology assessed using magnification narrow band imaging correlates well with histology in patients with suspected malabsorption syndrome. Dig Endosc. 2014;26:720–5.
29. Singh R, Nind G, Tucker G, Nguyen N, Holloway R, Bate J, et al. Narrow-band imaging in the evaluation of villous morphology: a feasibility study assessing a simplified classification and observer agreement. Endoscopy. 2010;42:889–94.
30. Yao K, Anagnostopoulos GK, Jawhari AU, Kaye PV, Hawkey CJ, Ragunath K. Optical microangiography: high-definition magnification colonoscopy with narrow band imaging (NBI) for visualizing mucosal capillaries and red blood cells in the large intestine. Gut Liver. 2008;2:14–8.
31. Kudo S, Hirota S, Nakajima T, Hosobe S, Kusaka H, Kobayashi T, et al. Colorectal tumors and pit pattern. J Clin Pathol. 1994;47:880–5.
32. Uraoka T, Saito Y, Ikematsu H, Yamamoto K, Sano Y. Sano's capillary pattern classification for narrow-band imaging of early colorectal lesions. Dig Endosc. 2011;23 Suppl. 1:112–5.
33. Matsuda T, Fujii T, Saito Y, Nakajima T, Uraoka T, Kobayashi N, et al. Efficacy of the invasive/non-invasive pattern by magnifying chromoendoscopy to estimate the depth of invasion of early colorectal neoplasms. Am J Gastroenterol. 2008;103:2700–6.